Study on the preparation and properties of talcum-fly ash based ceramic membrane supports

Chao Cheng
North China Electric Power University
Hongming Fu
North China Electric Power University
Heng Zhang (zhangchongheng@hotmail.com)
North China Electric Power University
Haiping Chen
North China Electric Power University
Dan Gao
North China Electric Power University

Research Article

Keywords: fly ash, ceramic membranes supports, water recovery, preparation

Posted Date: May 20th, 2020

DOI: https://doi.org/10.21203/rs.3.rs-29029/v1

Version of Record: A version of this preprint was published at Membranes on August 28th, 2020. See the published version at https://doi.org/10.3390/membranes10090207.

Study on the preparation and properties of talcum-fly ash based ceramic membrane supports

Chao Cheng, Hongming Fu, Heng Zhang *, Haiping Chen, Dan Gao

School of Energy, Power and Mechanical Engineering, North China Electric Power University, Beijing 102206, China

Corresponding author E-mail address: zhangchongheng@hotmail.com

ABSTRACT: Ceramic membrane method for moisture recovery from flue gas of thermal power plants is of considerable interest due to its excellent selection performance and corrosion resistance. However, manufacturing costs of commercial ceramic membranes are still relatively expensive, which promotes the development of new methods of preparing low-cost ceramic membranes. In this study, a method for the preparation of porous ceramic membrane supports is proposed. Low-cost fly ash from power plants is the main material of the membrane supports, and talcum is the additive. The fabrication process of the ceramic membrane supports is described in detail. The properties of the supports were fully characterized, including surface morphology, phase composition, pore diameter distribution and porosity. Corrosion resistance and mechanical strength of the supports were measured. The obtained ceramic membrane support displays a pore size of about 5 μm and porosity of 37.8%. Furthermore, the water recovery performance of the supports under different operating conditions was experimentally studied. The experimental results show that, the recovered water flux varies with operating conditions. In the study, the maximum recovered water flux reaches 5.22 kg/(m^2·h). The findings provide a guidance for the ceramic membrane supports application of water recovery from flue gas.

Keywords: fly ash; ceramic membranes supports; water recovery; preparation

1 Introduction

Currently, China is suffering serious water shortages and water pollution problems caused by, among others, rapid economic development [1]. In the industrial

sector, thermal power plants consume vast amount of water, accounting for about 11% of China's total industrial water consumption [2]. In short, China's water resources are limited, with a great demand for water and water conservation. In the case of air-cooled units alone in thermal power plants, water consumption of the wet desulfurization system accounts for more than 50% of the total water consumption of the units. However, water vapor discharged into the atmosphere along with the purified flue gas through the chimney accounts for more than 80% of the water consumption of those systems, with a large amount of this water vapor being generated in the coal combustion process. Moreover, a large amount of heat is discharged with flue gas. The content of water vapor in the flue gas discharged by a coal-fired power plant is 4–13%, while that discharged by a gas-fired power plant is more than 20%. A substantial amount of water can be conserved by recovering water vapor from flue gas [3]. Therefore, thermal power plants have huge water conservation potential [4].

Recovering water vapor and its gasification latent heat has attracted great interest in the scientific community over last few years, due to high moisture content in the flue gas of thermal power plants. General methods to recover moisture and its gasification latent heat include the condensation method and solution absorption method. The condensation method mainly adopts an indirect condensation heat exchanger [5], such as low temperature economizer [6], low pressure economizer [7,8], and direct contact condenser [9]. However, acid gas SO_2 exists in the flue gas that condense on the surface of the heat exchanger at lower temperature than the acid dew point, causing low-temperature corrosion, which seriously affects the service life and water recovery performance of the heat exchanger. The solution absorption method employs a solution with moisture absorption behavior as desiccant, such as lithium bromide, lithium chloride, calcium chloride solution, which directly contacts with flue gas promoting removal of flue gas moisture. Westerlund et al. [10] adopted two-stage absorption cycle system to remove flue gas particles and recycle the waste

heat in a biomass boiler. The absorber adopted packing type, divided into three stages to heat the return water using the recovered heat. At the same time, some hot flue gas is used for solution regeneration.

Considering the limitations of condensation heat exchanger that is susceptible to corrosion, the moisture recovery method of flue gas based on organic fiber membrane is preferred. The organic composite membrane is superior owing to low production cost, large surface area per unit volume, low weight, small floor area, and easy modularization. Chen et al. [11] prepared hydrophilic composite hollow fiber membrane sulfonated polyether ether ketone-polyether sulfone (SPEEK-PES) that possessed excellent thermal stability and mechanical properties. They also experimentally studied the effect of scavenging temperature and flow rate on membrane performance using simulated flue gas. The result showed that water recovery efficiency increased with the increase in temperature. Choi et al. [12] prepared TFC composite hollow fiber membrane via polymerization of 3,5-diaminobenzoic acid (DABA) aqueous solution and trimethyl chloride on the inner surface of PSF hollow fiber. The obtained membranes were used to create membrane modules, and the performance of the membrane module for recovering water under different operating conditions was studied experimentally. The maximum water flux of the membranes was 2.3 kg/(m^2·h), and the water recovery efficiency was 27.7%. Unfortunately, it is difficult to apply organic composite membranes to practical industry processes on large scale due to their low mechanical strength. Compared with hollow fiber membranes, inorganic ceramic composite membranes possess good mechanical properties to adhere to industrial requirements [13], and enhanced thermal stability, chemical stability and corrosion resistance of ceramic membranes ensuring their capability with high temperature and wide pH range [14]. In addition, the pore size of the ceramic membrane selection layer can be adjusted to compliment certain requirements, promoting excellent selectivity [15]. Wang et al.[16] proposed the recovering of waste heat and water from flue gas using nano-porous

ceramic membranes according to the capillary condensation principle. An engineering demonstration was carried out for industrial boiler flue gas waste heat and moisture recovery, the steam recovery efficiency reached 40% achieving good recovery performance. Chen et al. [3,17] studied the recovery performance of nanofiltration ceramic membranes of varied pore sizes under different experimental conditions. The ceramic membrane with 20 nm pore size is suitable for different flue gas conditions, with the highest water recovery efficiency of 55%. Gao et al. [18] designed a membrane module consisting of 46 porous ceramic membranes with a pore size of 1 μm and length of 40 cm. They studied its water and heat recovery performance in the flue gas from gas-fired boiler under different conditions, and maximum recovered water flux of 15.77 kg/(m^2·h).

Although ceramic membranes have excellent performance in flue gas moisture recovery, high production costs remains a major obstacle for large-scale application. Conventional ceramic membranes consisting of pure Al_2O_3, TiO_2, ZrO_2, SiO_2 or mixtures [13,19,20] require sinter temperature above 1500 °C. Expensive raw materials and large energy consumption during sintering results in high manufacturing cost of ceramic membranes [21,22]. At present, reports have shown the preparation of low-cost porous ceramic membrane using cheap traditional ceramic materials such as clay and kaolin. Elgamouz et al. [23] employed natural clay minerals as raw materials to prepare flat porous ceramic membrane supports of varied pore size by sintering at different temperatures, and coated them with tetra-ethyl orthosilicate by hydrothermal deposition. Mohammed et al. [24] used clay and $AlF_3 \cdot 3H_2O$ as raw materials to synthesize mullite based porous ceramic membranes at 1400°C sintering temperature. Hou et al. [25] added MoO_3 to the raw materials consisting of kaolin and Al_2O_3 to prepare mullite based ceramic membrane with a porosity of 67% and shrinkage of -2.57% at 1400°C sinter temperature.

Fly ash is a by-product of thermal production in power plants, which is currently employed in the cement industry [26]. But the application of fly ash for ceramic

membrane production is still in its infancy. Fang et al. [27] prepared tubular ceramic membrane supports with fly ash of different particle size distribution, with a coated selective layer. The average pore size and pure water flux obtained for ceramic membrane were 0.77 μm and 1.56×10^4 L/(m^2·h·bar), respectively. Zhu et al. [28] produced porous ceramic membranes with the main crystalline phase of mullite using fly ash as the raw material with the addition of different mass fraction of Al_2O_3. Qin et al. [29] applied ceramic membranes prepared with fly ash as precursor in juice clarification. Suresh et al. [30] employed fly ash, quartz and calcium carbonate to fabricate ceramic microfiltration membranes and evaluated membrane performances using synthetic oil-water emulsions. Zou et al. [31] used fly ash to prepare ceramic microfiltration membrane and used in oil-water emulsion treatment. Fu et al. [32] fabricated mullite ceramic membranes by using fly ash and $Al(OH)_3$ and MoO_3 and planned for water filtration. The above researches mainly focused on studying the influence of different factors on membrane preparation and the application in juice clarification, oil-water treatment, water filtration, etc., but less in flue gas water recovery.

In this study, low-cost fly ash based porous ceramic membranes supports were prepared and studied. The fly ash is the main raw material, and talc powder is the additive. Firstly, the supports were characterized by using scanning electron microscopy to observe the surface morphology of membrane supports, and utilizing mercury porosimeter to measure the pore diameter distribution. Besides, the mechanical strength and corrosion resistance were measured. Then, the water recovery performance of the fly ash based porous ceramic membrane supports from flue gas under different conditions (e.g. flue gas flow rate, flue gas temperature, cooling water flow rate, cooling water temperature) was experimentally studied. This article dedicates to prepare and study the low-cost ceramic membrane supports, and provides a guidance for flue gas moisture recovery application of ceramic membrane supports.

Nomenclature

A	initial surface area of the sample (m^2)	m_{in}	water vapor content in flue gas at the inlet (kg/h)
C	mass change on unit area of the sample (g/m^2)	m_{out}	water vapor content in flue gas at the outlet (kg/h)
d	inner diameter of the sample (mm)	S	membrane area (m^2)
D	outer diameter of the sample (mm)	y	The distance from the neutral axis (mm)
F	load when the sample breaks (N)	*Greek symbols*	
I	inertia moment of the section to the z axis(mm^4)	σ	bending strength(MPa)
J_{rec}	recovered water flux ($kg/(m^2 \cdot h)$)	η	water recovery efficiency (%)
L	spacing of the support blade (mm)	*Subscripts*	
M	moment (N· mm)	w	water
m_f	mass of the sample after corrosion (g)	in	inlet
m_i	mass of the sample before corrosion (g)	out	outlet

2 Experimental

2.1 Membrane preparation

Ceramic membrane supports were prepared using fly ash, which was produced by power plants, as the main material and talcum as the sintering aid. **Table 1** lists the main chemical composition of ceramic membrane supports raw materials. Carboxymethylcellulose and dextrin as the binder, and glycerin as the plasticizer were mixed with water in a certain proportion, and then added to the mixture of fly ash and talcum to form mud embryos, which were finally sintered into ceramic membrane supports. The specifications of raw materials used in this experiment are summarized in **Table 2**.

Table 1 Chemical composition of ceramic raw materials

Material	SiO_2	Al_2O_3	Fe_2O_3	CaO	MgO	Na_2O	K_2O	SO_3	Loss of ignition
Fly ash	50.6	27.1	7.1	2.8	1.2	0.5	1.3	0.3	8.2

Talcum	58	20	--	1.8	18	--	--	--	--

Table 2 Raw materials of ceramic membrane supports

Materials	Specifications	Sources
Fly ash	100 Mesh	A power plant of China Datang corporation
Talcum	3000 Mesh industrial grade	Shijiazhuang, Hebei
Carboxymethylcellulose	Industrial grade high viscosity	Cangzhou, Hebei
Dextrin	Industrial grade high viscosity	Ji'nan, Shandong
Glycerin	99% Purity	A chemical plant in Beijing

In this paper, ceramic membrane supports was prepared by extrusion method, which is a common method of tubular ceramic membrane preparation [33-36]. The specific preparation process of the support is as follows: The pretreated fly ash, talc powder and other ceramic additives were mixed by a mixer (HL-5) and stirred uniformly with appropriate amount of water. After being refined 2–3 times by a vacuum pugging machine, the mixture was staled for 24 h at 30 °C. Then the green bodies were refined for 3–4 times again to obtain sufficient strength and shape. The wet green bodies of fly ash based ceramic membrane were obtained by extruding the green bodies using an extruder (LWJ63). The wet green bodies without deformation or crake were aligned by a straightening machine (XZJ-25/1000) and dried for 48 h, generating the green body of the fly ash based tubular ceramic membrane supports during the process. Then, under the premise of ensuring that the sintering does not crack and the layer is continuous, the tubular fly ash based ceramic membranes were obtained by sintering at appropriate sintering parameters in a high temperature pipe furnace (TSK-8-14). The concrete operational process is shown in **Fig. 1**.

The pretreatment of fly ash is mainly to remove large particles of fly ash and impurities, so that the size of fly ash particles is uniform. As a sintering aid, talc powder could be used as a magnesium source supplement due to its high magnesium

content, which could make the density uniform and surface smooth of the membrane supports after sintering. The purpose of vacuum pugging is to eliminate the uneven components and moisture in fly ash mixture. Through staling, the mixture of fly ash, talcum, and water is kept uniformly mixed. The green bodies extruded by the straightener is in the form of wet body, deform during the extrusion process. It needs to be straightened to ensure that the membrane supports produced is relatively straight. After drying, sintering is carried out. At last, the membrane supports are pretreated and cleaned with deionized water and distilled water to remove water-soluble impurities.

2.2 Characterization method

The pore size of fly ash used in this experiment was measured by Laser Scattering Particle Size Distribution Analyzer (LA-960, Horiba, France). X-ray diffraction (XRD, AL-Y3000, Aolong, China) was used to analyze the phase composition of fly ash and the phase composition of the ceramic membrane supports. To determine the appropriate sintering parameters, the green bodies were analyzed by a thermogravimetric analyzer (TGA-1450A, Innuo, China). The surface morphology of the ceramic membrane supports was observed by a scanning electron microscopy (JSM6490LV, JEOL, Japan). The pore size and porosity of the support were examined using a mercury porosimeter (Poremaster 60, Anton-Paar, America), and its mechanical strength was measured using the three point bending method. Furthermore, the corrosion resistance test was carried out considering the practical application of support in flue gas dehydration.

The method for measuring the bending strength is shown in **Fig. 2**. Since the sample of 120 mm is tubular and the bending head is a cylinder surface, contact of the intermediate force point is the point contact, resulting in much lower measured bending strength than the actual value.

The bending strength calculation formula is as follows:

$$\sigma = \frac{M \cdot y}{I_z} = \frac{(1/4 \cdot FL) \cdot D/2}{\pi\left(D^4 - d^4\right)/64} \quad (1)$$

where, σ is the bending strength; M is the moment; I_Z is the inertia moment of the section to the z axis; F is the load when the sample breaks; L is the spacing of the support blade; D and d are the outer and inner diameter of the sample, respectively.

The corrosion resistance measurement method is as follows: sulfuric acid solution with a mole fraction of 3 mol/L was prepared using analytically pure sulfuric acid and deionized water. The sample was immersed in the sulfuric acid solution at slight boiling state for 24 h. After, the sample was washed by deionized water and completely dried at a constant temperature prior to measurement.

The formula for calculating the mass change on unit area before and after corrosion is as follows:

$$C = \frac{\left|m_f - m_i\right|}{A} \quad (2)$$

where, C is the mass change on unit area of the sample; m_f and m_i are the mass of the sample before and after corrosion, respectively; A is initial surface area of the sample.

2.3 Dehydration experiment of flue gas

2.3.1 Experimental devices

The simulated flue gas dehydration experiment was carried out with the self-made fly ash based ceramic membrane supports. The length, outer diameter, inner diameter, and effective membrane area of the self-made fly ash based ceramic membrane supports are 80 cm, 12 mm, 8 mm and, 0.029 m^2, respectively. The experimental system diagram is shown in **Fig. 3**.

As shown in **Fig. 3**, the whole experimental system consists of a flue gas system and cooling water system. The flue gas, composed of nitrogen and water vapor, is prepared artificially. The simulated flue gas is introduced into the shell side of the membrane module and passes through the outside of the membrane tube, while water

flows inside the membrane tube for cooling down the tube. Flue gas and water flows counter-currently. In order to avoid heat loss, membrane module housing and pipes are treated with insulating cotton.

Flue gas flow rate is controlled by a mass flow controller. Nitrogen first enters a humidifier of a specific temperature through the mass flow controller, then enters the membrane module and scours membrane tube, and finally discharges to the atmosphere. The humidifier is heated by a water bath with adjustable temperature. The temperature and relative humidity of flue gas at the inlet and outlet of the membrane module are measured by a temperature and humidity transmitter. The relative humidity (RH) of simulated flue gas is about 100%.

In terms of cooling water, water is pumped out of the constant temperature water tank by the self-priming pump flowing through the membrane tube and entering the return tank. The inlet and outlet temperature of cooling water are measured, respectively, by thermocouples set at the inlet and outlet of membrane tube. Cooling water flow rate is controlled by a flow meter. The relative vacuum is about −20 kPa in experiments.

Under the action of cooling water, after the hot flue gas enters the membrane module, when flue gas scours the membrane tube with lower temperature, water vapor condenses on the surface of the membrane tube, and the condensed droplets enters the membrane tube along pores and discharges with the cooling water. The experimental apparatus used in the experiment are tabulated in **Table 3**.

Table 3 Parameters of experimental apparatus

Experimental apparatus	Model	Parameters	Precision	Manufacturer
Gas flow controller	D07-9E	30 SLM	±2 %	Beijing Sevenstar,China
Temperature and humidity transmitter	TH-21E	Temperature Range: –40 °C to 125 °C RH Range: 0–100%	≤±0.2 °C ≤±2 %	Guangzhou Anymetre,China
Eight-loop digital display device	HT-MK807-01-23-KL	-	0.5 % FS	Hantang Precision Instrument,China

Thermocouple	PT100	–50 °C to 200 °C	A Class	Hangzhou Sinomeasure, China
Miniature electric diaphragm pump	PLD-1205	Max flow rate:3.2 L/min	-	Shijiazhaung Pulandi, China
Flow meter	LZT-M15	Range:0.2–2.0 LPM	≤±4 %	VAKADA, China

2.3.2 Experimental performance evaluation

The recovered water flux and water recovery efficiency were the main indicators of water recovery performance.

The recovered water flux was calculated as follows:

$$J_{rec} = \frac{m_{in} - m_{out}}{S} \tag{3}$$

where J_{rec} is the recovered water flux, kg/(m^2·h); m_{in} and m_{out} are the water vapor content in flue gas flow at the inlet and outlet of membrane module, respectively, kg/h; and S is the membrane area, m^2.

The water recovery efficiency was given by

$$\eta_w = 1 - \frac{m_{out}}{m_{in}} \tag{4}$$

where η_w is the water recovery efficiency, %.

2.4 Uncertainty analysis

The testing uncertainty may cause experimental errors. Uncertainty analysis was performed in order to preserve the accuracy of experimental results in the study. The direct testing parameters contain flue gas flow rate $Q_{N_2,in}$ and $Q_{N_2,out}$, relative humidity φ_{in} and φ_{out},

The relative uncertainty of the recovered water flux ΔJ_w was computed from

$$\Delta J_w = \frac{\sqrt{\left(\frac{\partial J_w}{\partial Q_{N_2,in}}\Delta Q_{N_2,in}\right)^2 + \left(\frac{\partial J_w}{\partial \varphi_{in}}\Delta\varphi\right)^2 + \left(\frac{\partial J_w}{\partial \varphi_{out}}\Delta\varphi\right)^2 + \left(\frac{\partial J_w}{\partial Q_{N_2,out}}\Delta Q_{N_2,out}\right)^2}}{J_w} \tag{4}$$

Through calculation, the maximum relative uncertainty of the recovered water flux ΔJ_w is 3.56%.

3 Results and Discussion

3.1 Characterization of raw materials

SEM image of fly ash after pretreatment and its particle size analyzed by laser particle sizer are shown in **Fig.** 4 and **Fig. 5**, respectively. The particle size distribution of fly ash is between 1–10 μm with an average particle size of 3.29 μm. According to SEM image, most fly ash particles are spherical, their chemical composition are mainly alumina and silica, which is suitable for the preparation of ceramic membrane supports.

XRD diffraction pattern of fly ash is shown in **Fig. 6**. The fly ash phase compositions mainly contain mullite ($Al_6Si_2O1_3$; PDF#15-0776), sillimanite (Al_2SiO_5; PDF#38-0471) and corundum (Al_2O_3; PDF#46-1212). The slight bulge at small angle of the diffraction peak indicates that the raw material contains a large amount of amorphous silicon glass phase.

The thermogravimetric analysis of the green body using 10 °C/min heating rate in an air atmosphere is shown in **Fig. 7**. The results indicate that free water is removed at about 100 °C while some bound water is removed at about 200 °C. Decomposition of the binder promotes an exothermic reaction at about 350 °C, resulting in a small temperature change in the differential thermal analysis. However, insignificant weight loss is observed at this temperature. Above 700 °C, the differential thermal analysis temperature is greater than that at ambient temperature due to combustion of the remaining carbon particles inside the material and the decomposition of the organic additive. According to the thermal analysis results, the sintering parameters are determined preliminarily, the results are shown in **Fig. 8**.

The thermogravimetric analysis results reveals an obvious weight loss of the ceramics at 135 and 350 °C. Thus, it is necessary to adopt heat preservation to ensure

complete removal of adsorbed water and combined water. A lower temperatures rise rate was adopted between 600 and 900 °C to allow the burnout of pore forming agents in ceramics. When the temperature reaches 1200 °C, it is maintained for 3 h to increase the densification degree of ceramic crystal and the strength of support.

3.2 Characterization of fly ash based ceramic membrane supports

The self-made ceramic membrane supports was characterized. Scanning electron microscopy was used to observe the surface morphology of the membrane supports. The XRD diffraction pattern was used to characterize the phase composition of the membrane supports. Mercury porosimeter was used to measure the pore diameter distribution of the membrane supports.

Fig. 9 depict scanning electron microscopy images of the surface of fly ash-based ceramic membrane supports under 2000 and 5000 times magnification, respectively. As shown, the grains of the support are uniform and distributed in blocks. The support surface is rough and dense, without obvious defects.

Fig. 10 describes the XRD diffraction pattern of fly ash based ceramic membrane supports. The results indicate that the main crystal phases of the ceramic membrane supports are anorthite ($CaAl_2Si_2O_8$; PDF#41-1486) and ringwoodite ($(Mg/Fe)_2SiO_4$; PDF#21-1258). A slight bulge of the diffraction peak at the small angle shows that the anorthite phase is an amorphous phase, and the nonexistent of cordierite phase may be caused by insufficient sintering temperature.

Fig. 11 illustrates the mercury adsorption curve of the support, where the pore size of the talcum-fly ash based ceramic membrane supports is concentrated at 5–10 μm. **Fig. 12** shows the pore size distribution curve and pore size distribution histogram diagram of talcum-fly ash based ceramic membrane supports, respectively. Both figures indicate that pore size of talcum-fly ash based ceramic membrane supports is relatively concentrated, near 5 and 9 μm, with porosity of 37.8%.

Ref. [37] pointed out that when the pore size of the hydrophilic membrane is in the range of 2–50 nm, capillary condensation occurs, indicating that the water vapor is

more likely to condense in the pores. Wang et al. [38] pointed out that because of capillary condensation, components of CO2, NOx, and SO2 etc were inhibited entering the membrane due to its high selectivity. However, Kim et al. [39] was skeptical about whether capillary condensation occurs, and suggested that the transmembrane mode may be a competition between water vapor condensation and SOx adsorption. Our previous study [40] results indicated that SO_2 could condense then penetrate into the membrane. The aforementioned researches are all using microporous membranes. Li et al. [41] said that the vapor directly condensed on the surface of the membrane and then penetrated into the membrane when the pore size is greater than 1 μm. It's worth noting that the pore diameter of the support in this paper reaches 5–10 μm, thus the water vapor does not undergo capillary condensation in the pores. The gas molecular diameter in the flue gas is in the order of nanometer. Other gas components in the flue gas may condense first and then penetrate into the membrane through the membrane pores. What's more, a small amount of noncondensable gas may also enter the membrane under the effect of pressure difference.

The change of the mass on unit area and bending strength of the talcum-fly ash based ceramic membrane supports after corrosion are shown in **Fig. 13** and **Fig. 14**, respectively. The self-made ceramic membrane mass changes greatly after corrosion, showing that the excellent bending property sharply decreases to less than 10 MPa after the corrosion test. This result is consistent with the conclusions in Ref. [42].

It can be seen from **Table 1** that the main component of fly ash is SiO_2, Al_2O_3, Fe_2oO_3, and CaO. To the best of our knowledge, however, these components react with sulfuric acid, and the reaction formula is shown as Eqs. (5) and (6) [43]. Therefore, when sulfuric acid solution is used for corrosion, the prepared supports reacts with sulfuric acid to generate sulfuric acid mineral salt, and the corrosion part of the support gradually soften, and even crack. In addition, sulfuric acid solution could also cause the degradation of binder and plasticizer. Consequently, the

mechanical strength of the support decreases after sulfuric acid corrosion, leading to the fracture of the supports during the installation of membrane module for flue gas moisture recovery, and shorten its service life.

$$xCaO \cdot ySiO_2 \cdot zH_2O + SO_4^{2-} + 2H_2O \rightarrow CaSO_4 \cdot 2H_2O + Si(OH)_4 \quad (5)$$

$$\begin{aligned} &3CaO \cdot Al_2O_3 \cdot CaSO_4 \cdot 12H_2O + 2CaSO_4 \cdot 2H_2O + 16H_2O \\ &\rightarrow 3CaO \cdot Al_2O_3 \cdot 3CaSO_4 \cdot 32H_2O \end{aligned} \quad (6)$$

3.3 Flue gas dehydration experiment results

Fig. 15 shows the effect of flue gas flow rate on flue gas water recovery performance. As the flue gas flow rate increases, the recovered water flux also increases, but the water recovery efficiency decreases significantly with increasing flue gas flow rate. This is because when the relative humidity of the flue gas remains constant, water vapor content increases proportionally with the increase of flue gas flow, thus, the recovered water flux increases with the increase of flue gas flow rate. However, an increase of flue gas flow leads to elevation of flow velocity, promoting the water vapor in flue gas to discharge with flue gas before being recovered, thus decreasing water recovery efficiency.

The influence of flue gas temperature on water recovery performance is shown in **Fig. 16**. When flue gas temperature increases from 40 to 70 °C, the recovered water flux and water recovery efficiency increases from 0.74 to 5.22 kg/(m^2·h) and 64.8% to 81.4%, respectively. As shown in **Fig. 16**, with flue gas temperature increases, the recovered water flux increases in an approximate parabolic form. That is, the higher the flue gas temperature, the faster the growth rate of recovered water flux, due to the water vapor content increases exponentially with increasing the flue gas temperature at a certain flow rate. However, flue gas enthalpy value increases with the increase of flue gas temperature. When the cooling water flow rate and temperature are fixed, the uncondensed water vapor increases correspondingly. Although the recovered water flux increases more rapidly, the growth trend of water recovery efficiency is more and

more slower.

Effect of cooling water flow rate on water recovery performance is shown in **Fig. 17**. At 50 °C flue gas temperature and 20 °C cooling water temperature, an increase in cooling water flow rate slightly influences the water recovery of the flue gas. When the cooling water flow increases from 0.5 to 2 L/min, the water recovery flux is approximately 1.50 kg/(m^2·h), while the water recovery efficiency increases slightly from 73.6% to 74.3%. In our previous study [17], the recovered water flux and water recovery efficiency increase with increasing cooling water flow rate. Nevertheless, when the flue gas flow rate flowing into membrane module is constant, the continuous increase of cooling water shows an insignificant affect on recovered water flux and water recovery efficiency as a result of the condensation of all recyclable water in the flue gas.

Fig. 18 displays the effect of cooling water temperature on water recovery performance. When the cooling water temperature increases from 15 to 25 °C, recovered water flux decreased from 1.66 to 1.50 kg/(m^2·h), and water recovery efficiency decreases from 79.7 to 73.0%. When the cooling water temperature increases, the temperature difference between the cooling water and flue gas decreases, the heat transfer capacity decreases, and the cooling effect deteriorates, leading to the decrease of condensation rate of water vapor. A large amount of water vapor is discharged from the membrane module without condensation. As a result, recovered water flux decreases, and water recovery efficiency accordingly decreases.

Compared with other studies, the ceramic membranes manufactured by fly ash [27,29], kaolin [20] and clay [24] are mostly used for juice clarification [29], oil-water emulsion treatment [31], and are currently less used for flue gas moisture recovery. Chen et al. [3] carried out experimental study on 20 nm membrane tube by vacuum pumping method, when the flue gas temperature reached 70 ℃, the recovered water was higher than 1 kg/(m^2·h). Gao et al. [18] used membrane modules to conduct research in actual gas-fired flue gas, and the maximum recovered water was 15.77

kg/(m^2·h). The maximum recovered water is higher than that in this article, this is because the ratio of flue gas flow rate to membrane area in [18] was 2286 m^3/h/m^2, which was much greater than 18 m^3/h/m^2 in this article. Whereas, commercial membranes were used in Ref. [3,18], which is usually made of alumina, with high cost of raw materials [44]. In addition, the manufacturing process of commercial membrane is complicated, which requires relatively high sintering temperature (up to 1500 °C) [45]. Low-cost ceramic membranes used fly ash, kaolin, and clay as raw materials, alumina as auxiliary materials, and MoO_3 and talc powder as additives could significantly reduce its manufacturing cost [21].

4 Conclusion

In this study, ceramic membrane supports were successfully prepared using fly ash, talc powder, and appropriate amount of carboxymethyl cellulose and dextrin as raw material, sintering aid, and pore former, respectively. The pore size distribution of the obtained ceramic membranes is near 5 and 9 μm, with 37.8% porosity. Anorthite and ringwoodite are the main crystalline phase. The bending strength of the obtained ceramic membranes with excellent bending behavior decreases below 10 MPa after strong-acid corrosion. The ceramic membrane supports can be regarded as a macroporous membrane due to its pore size.

The experimental results of moisture recovery from flue gas using self-made supports show that, with the increase of flue gas flow rate, recovered water flux increases linearly, while water recovery efficiency is the opposite. Both recovered water flux and water recovery efficiency increases with increasing flue gas temperature, and decreases with increasing cooling water temperature. The recovered water flux can reach up to 5.22 kg/(m^2·h) when flue gas temperature is 70 °C. With the increase of cooling water flow rate, the recovered water flux is almost unchanged.

In the future, improving the corrosion resistance and mechanical strength of the fly ash based ceramic membrane supports will be the focus of this research. And

applying the supports to the field of flue gas moisture recovery in coal-fired power plants is planned to be further explored.

Acknowledgements

This work is financially supported by National Key R&D Program of China (2018YFB0604302) and the Fundamental Research Funds for the Central Universities (JB2019097).

References

[1] Zhu Z, Dou J. Current status of reclaimend water in China: an overview. *J Water Reuse Des* 2018, 8(3):293-307.
[2] Zhang X, Liu J, Tang Y*, et al.* China's coal-fired power plants impose pressure on water resources. *J Clean Prod* 2017, 161:1171-9.
[3] Chen H, Zhou Y, Su X*, et al.* Experimental study of water recovery from flue gas using hollow micro-nano porous ceramic composite membranes. *J Ind Eng Chem* 2018, 57:349-55.
[4] Shao W, Feng J, Liu J, Yang G, Yang Z, Wang J. Research on the Status of Water Conservation in the Thermal Power Industry in China. *Energy Procedia* 2017, 105:3068-74.
[5] Li Y, Yan M, Zhang L*, et al.* Method of flash evaporation and condensation – heat pump for deep cooling of coal-fired power plant flue gas: Latent heat and water recovery. *Appl Energ* 2016, 172:107-17.
[6] Xu G, Xu C, Yang Y, Fang Y, Li Y, Song X. A novel flue gas waste heat recovery system for coal-fired ultra-supercritical power plants. *Appl Therm Eng* 2014, 67(1-2):240-9.
[7] Wang C, He B, Sun S*, et al.* Application of a low pressure economizer for waste heat recovery from the exhaust flue gas in a 600MW power plant. *Energy* 2012, 48(1):196-202.
[8] Wang C, He B, Yan L, Pei X, Chen S. Thermodynamic analysis of a low-pressure economizer based waste heat recovery system for a coal-fired power plant. *Energy* 2014, 65:80-90.
[9] Zhao X, Fu L, Wang X, Sun T, Wang J, Zhang S. Flue gas recovery system for natural gas combined heat and power plant with distributed peak-shaving heat pumps. *Appl Therm Eng* 2017, 111:599-607.
[10] Westerlund L, Hermansson R, Fagerström J. Flue gas purification and heat recovery: A biomass fired boiler supplied with an open absorption system. *Appl Energ* 2012, 96(3):444-50.
[11] Chen H, Zhou Y, Sun J*, et al.* An experimental study of membranes for capturing

water vapor from flue gas. *J Energy Inst* 2017, 91(3):1-10.
[12]Choi O, Ingole PG, Lee H-K. Preparation and characterization of thin film composite membranefor the removal of water vapor from the flue gas at bench scale. *Sep Purif Technol* 2019, 211:401-7.
[13]Li S, Wang CA, Zhou J. Effect of starch addition on microstructure and properties of highly porous alumina ceramics. *Ceram Int* 2013, 39(8):8833–9.
[14]Dong Y, Lin B, Zhou J-e*, et al.* Corrosion resistance characterization of porous alumina membrane supports. *Mater Charact* 2011, 62(4):409-18.
[15]Monash P, Pugazhenthi G. Effect of TiO2 addition on the fabrication of ceramic membrane supports: A study on the separation of oil droplets and bovine serum albumin (BSA) from its solution. *Desalination* 2011, 279(1-3):104-14.
[16]Wang D, Bao A, Kunc W, Liss W. Coal power plant flue gas waste heat and water recovery. *Appl Energ* 2012, 91(1):341-8.
[17]Chen H, Zhou Y, Cao S*, et al.* Heat exchange and water recovery experiments of flue gas with using nanoporous ceramic membranes. *Appl Therm Eng* 2017, 110:686-94.
[18]Gao D, Li Z, Zhang H, Chen H. Moisture Recovery From Gas-fired Boiler Exhaust Using Membrane Module Array. *J Clean Prod* 2019, 231:1110-21.
[19]Wei Z, Jie H, Zhu Z. High-aluminum fly ash recycling for fabrication of cost-effective ceramic membrane supports. *J Alloy Compd* 2016, 683:474-80.
[20]Hubadillah SK, Othman MHD, Matsuura T*, et al.* Fabrications and applications of low cost ceramic membrane from kaolin: A comprehensive review. *Ceram Int* 2018, 44(5):4538-60.
[21]Mestre S, Gozalbo A, Lorente-Ayza MM, Sánchez E. Low-cost ceramic membranes: A research opportunity for industrial application. *J Eur Ceram Soc* 2019, 39(12):3392-407.
[22]Dong Y, Zhou J-e, Lin B*, et al.* Reaction-sintered porous mineral-based mullite ceramic membrane supports made from recycled materials. *J Hazard Mater* 2009, 172(1):180-6.
[23]Abdelaziz E, Najib T. From a naturally occurring-clay mineral to the production of porous ceramic membranes. *Micropor Mesopor Mat* 2018, 271(5):52-8.
[24]Rashad M, Balasubramanian M. Characteristics of porous mullite developed from clay and AlF3·3H2O. *J Eur Ceram Soc* 2018, 38(10):3673-80.
[25]Hou Z, Cheng L, Liangliang L, Shaowei Z. Microstructural evolution and densification behavior of porous kaolin-based mullite ceramic added with MoO_3. *Ceram Int* 2018, 44(15):17914-8.
[26]Gonzalez A, Navia R, Moreno N. Fly ashes from coal and petroleum coke combustion: current and innovative potential applications. *Waste Manage* 2009, 27(10):976-87.
[27]Fang J, Qin G, Wei W, Zhao X. Preparation and characterization of tubular supported ceramic microfiltration membranes from fly ash. *Sep Purif Technol* 2011, 80(3):585-91.

[28] Zhu J, Hong Y. Microstructure and properties of mullite-based porous ceramics produced from coal fly ash with added Al_2O_3. *Int J Min Met Mater* 2017, 24(3):309-15.
[29] Qin G, Lü X, Wei W, Li J, Cui R, Hu S. Microfiltration of kiwifruit juice and fouling mechanism using fly-ash-based ceramic membranes. *Food BioprodProcess* 2015, 96:278-84.
[30] Suresh K, Pugazhenthi G, Uppaluri R. Fly ash based ceramic microfiltration membranes for oil-water emulsion treatment: Parametric optimization using response surface methodology. *J Water Process Eng* 2016, 13:27-43.
[31] Zou D, Qiu M, Chen X, Drioli E, Fan Y. One step co-sintering process for low-cost fly ash based ceramic microfiltration membrane in oil-in-water emulsion treatment. *Sep Purif Technol* 2019, 210:511-20.
[32] Fu M, Liu J, Dong X, Zhu L, Dong Y, Hampshire S. Waste recycling of coal fly ash for design of highly porous whisker-structured mullite ceramic membranes. *J Eur Ceram Soc* 2019, 39(16):5320-31.
[33] Dong Y, Chen S, Zhang X, Yang J, Liu X, Meng G. Fabrication and characterization of low cost tubular mineral-based ceramic membranes for micro-filtration from natural zeolite. *J Membrane Sci* 2006, 281(1-2):592-9.
[34] Dong Y, Liu X, Ma Q, Meng G. Preparation of cordierite-based porous ceramic micro-filtration membranes using waste fly ash as the main raw materials. *J Membrane Sci* 2006, 285(1/2):173-81.
[35] Jedidi I, Khemakhem S, Sa?Di S*, et al.* Preparation of a new ceramic microfiltration membrane from mineral coal fly ash: Application to the treatment of the textile dying effluents. *Powder Technology* 2011, 208(2):427-32.
[36] Hedfi I, Hamdi N, Rodriguez MA, Srasra E. Development of a low cost micro-porous ceramic membrane from kaolin and Alumina, using the lignite as porogen agent. *Ceram Int* 2015, 42(4):5089-93.
[37] Horikawa T, Do DD, Nicholson D. Capillary condensation of adsorbates in porous materials. *Adv Colloid Interface* 2011, 169(1):40-58.
[38] Wang D, Bao A, Kunc W, Liss W. Coal power plant flue gas waste heat and water recovery. *Appl Energ* 2012, 91:341–8.
[39] Kim JF, Park A, Kim S-J*, et al.* Harnessing clean water from power plant emissions using membrane condenser technology. *ACS Sustain Chem Eng* 2018, 6:6425-33.
[40] Cheng C, Zhang H, Chen H. Experimental study on water recovery and SO_2 permeability of ceramic membranes with different pore sizes. *Int J Energy Res* 2020:1–12.
[41] Li Z, Zhang H, Chen H, Zhang J, Cheng C. Experimental research on the heat transfer and water recovery performance of transport membrane condenser. *Appl Therm Eng* 2019, 160:114060.
[42] Wei Z, Xiao Y, Tao Y, Zuhua Z. The degradation mechanisms of alkali-activated fly ash/slag blend cements exposed to sulphuric acid. *Constr Build Mater* 2018,

186:1177-87.
[43] Khan HA, Castel A, Khan MSH. Corrosion investigation of fly ash based geopolymer mortar in natural sewer environment and sulphuric acid solution. *Corros Sci* 2020, 168:108586.
[44] Wei Z, Hou J, Zhu Z. High-aluminum fly ash recycling for fabrication of cost-effective ceramic membrane supports. *J Alloy Compd* 2016, 683:474-80.
[45] Li L, Chen M, Dong Y*, et al.* A low-cost alumina-mullite composite hollow fiber ceramic membrane fabricated via phase-inversion and sintering method. *J Eur Ceram Soc* 2016, 36(8):2057-66.

Figures

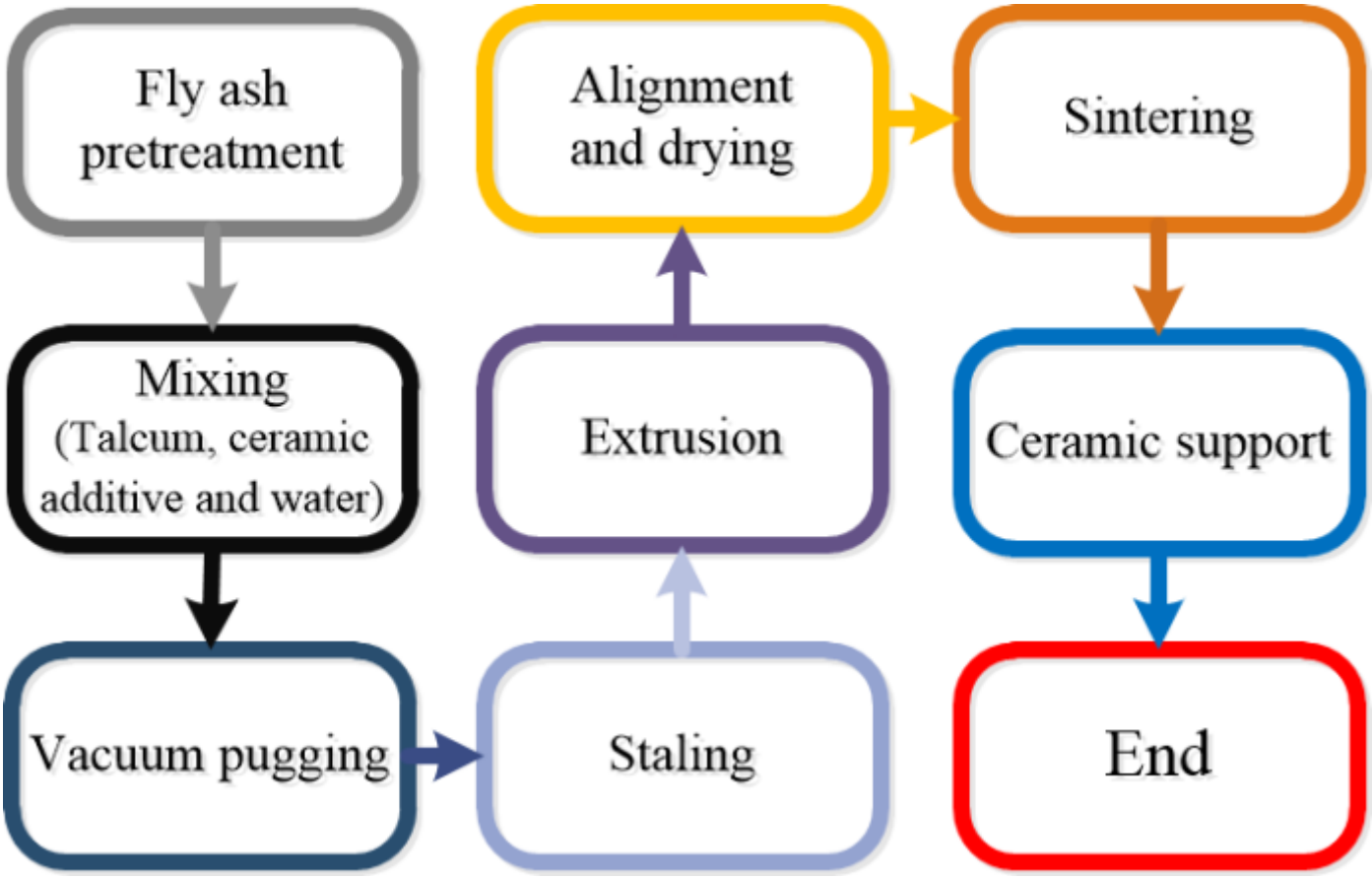

Figure 1

Fly ash based ceramic membrane supports preparation process

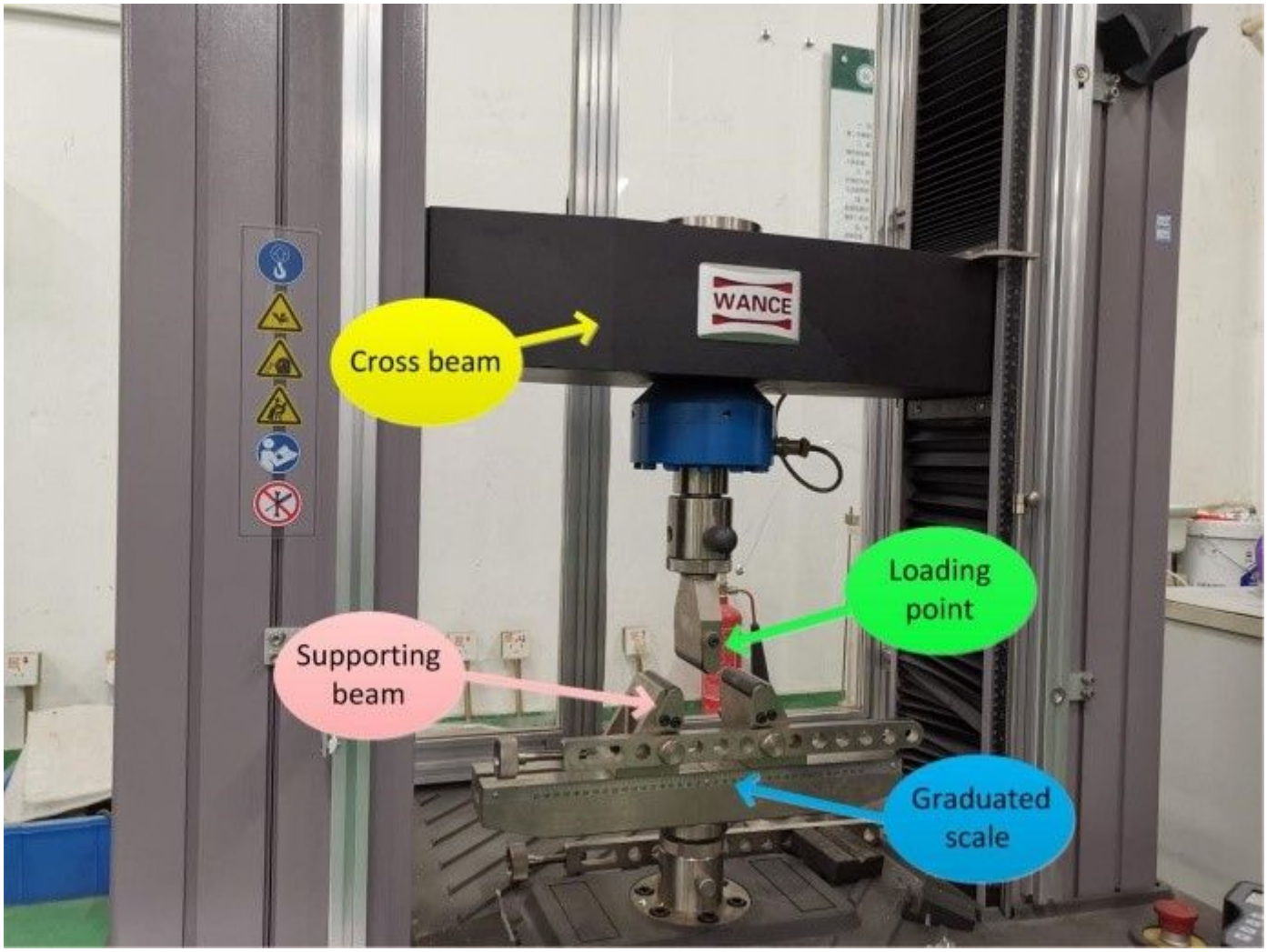

Figure 2

Three-point bending experimental setup

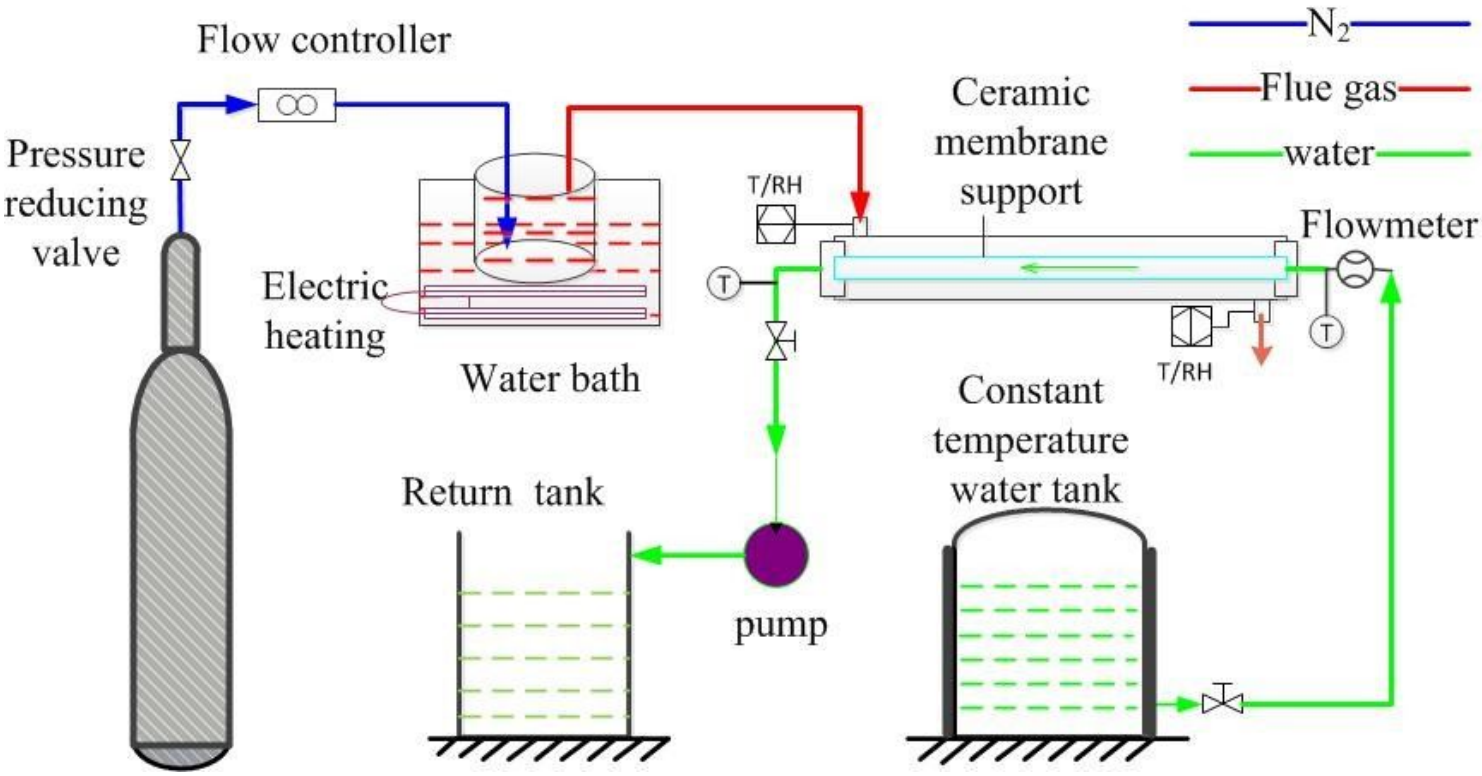

Figure 3

Diagram of the flue gas water recovery experimental system

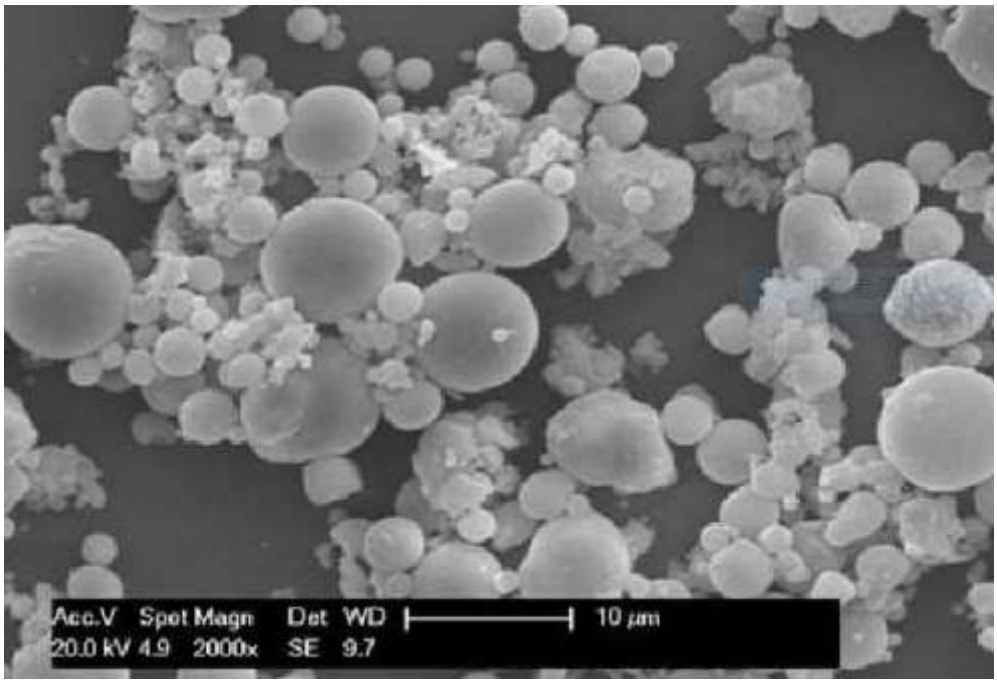

Figure 4

SEM image of fly ash

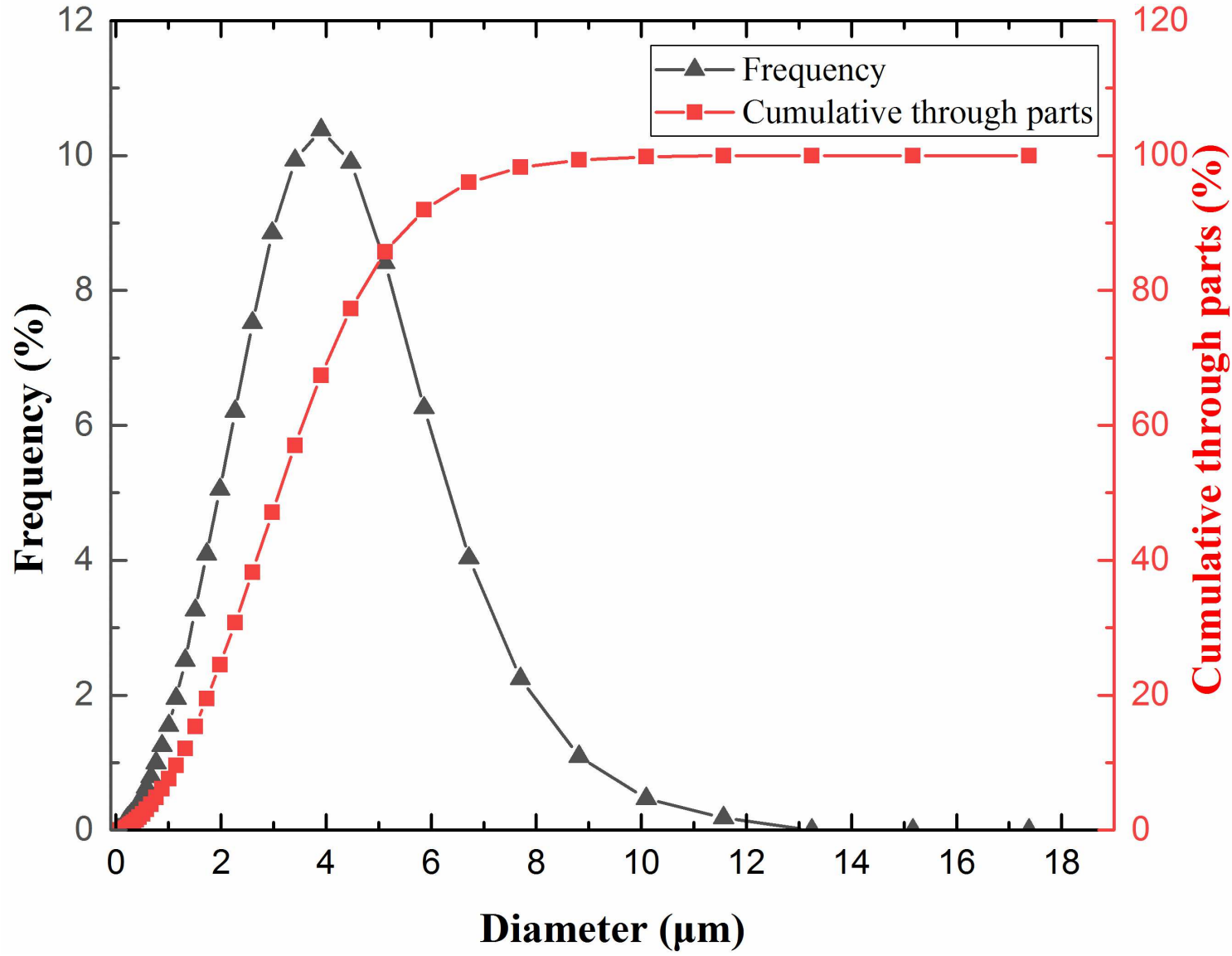

Figure 5

Particle size distribution of fly ash

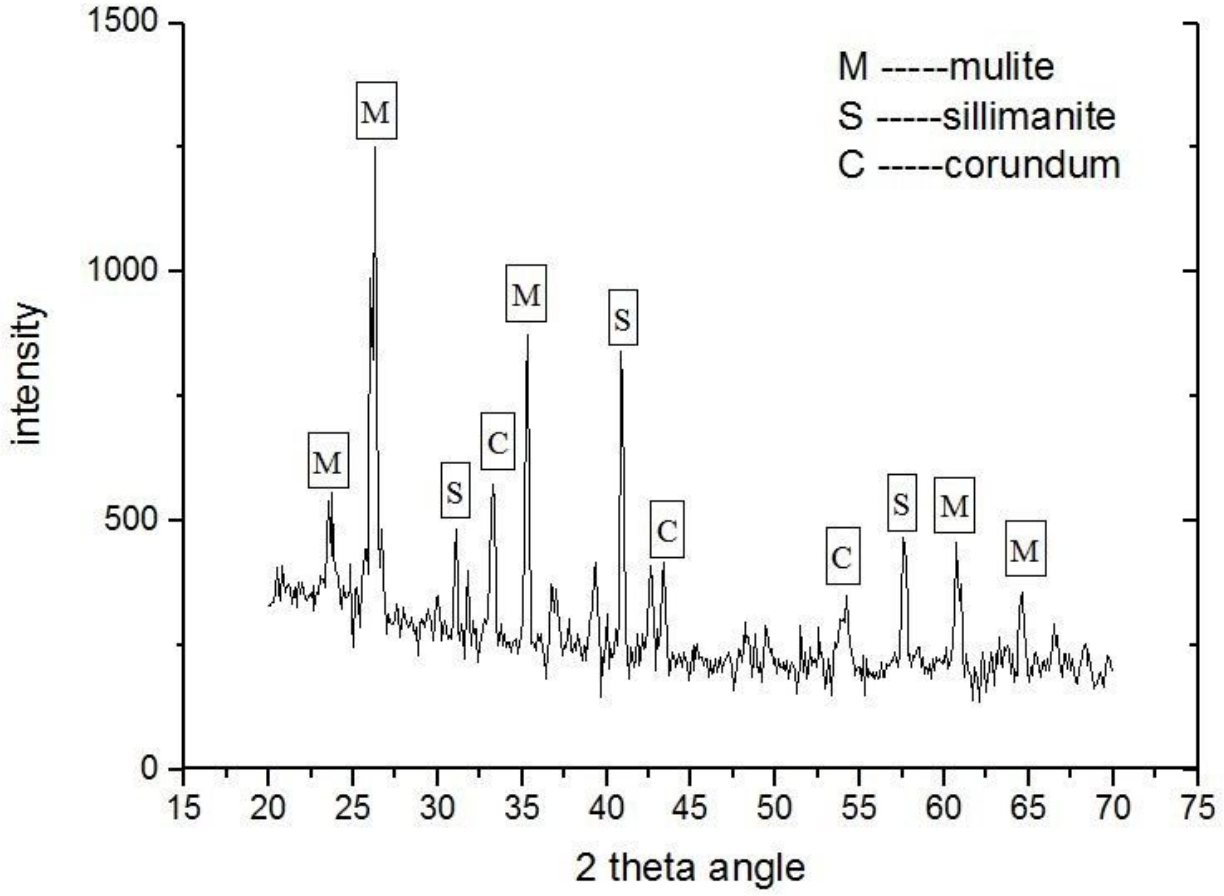

Figure 6

XRD diffraction pattern of fly ash

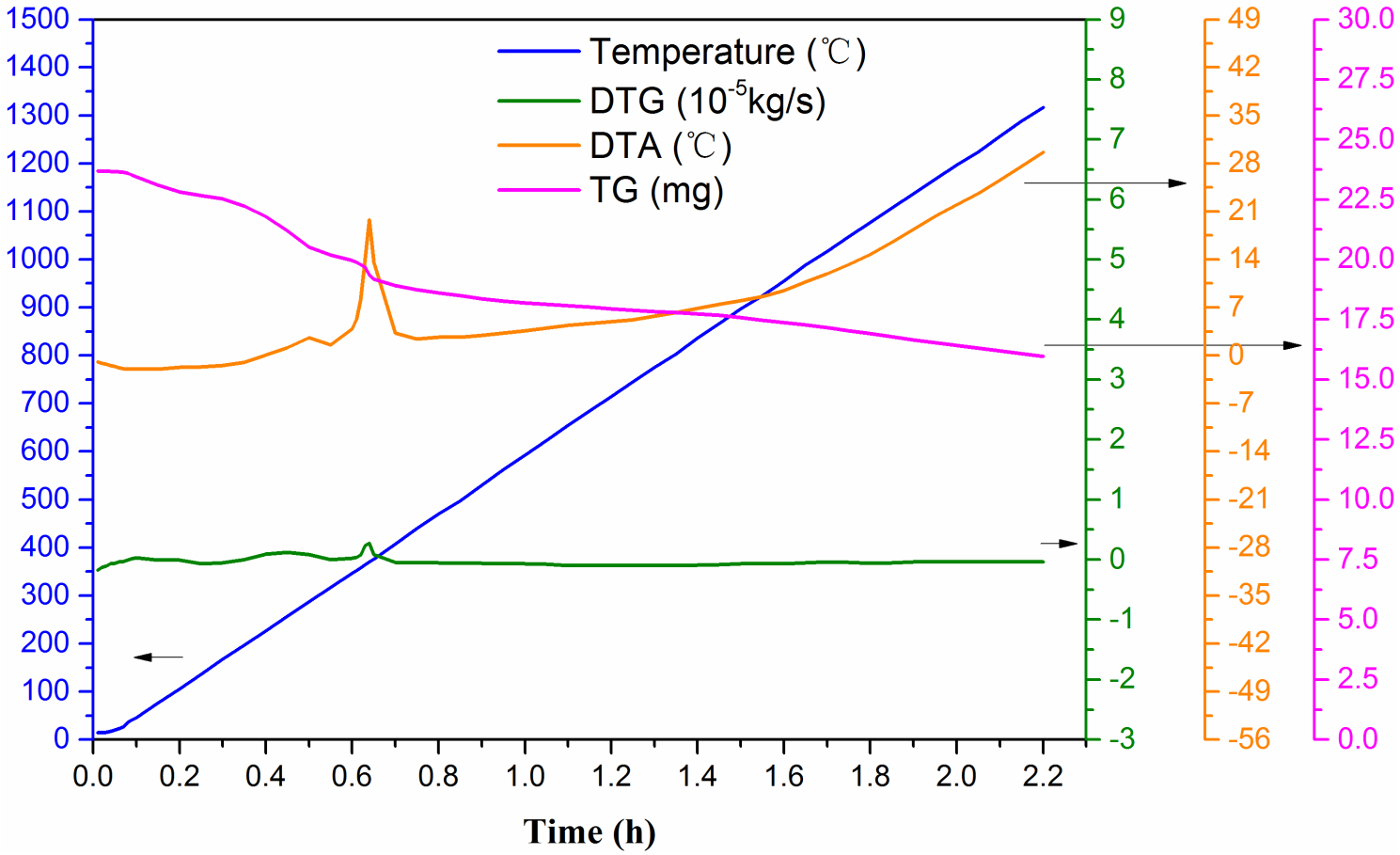

Figure 7

Thermogravimetric analysis curve of green body

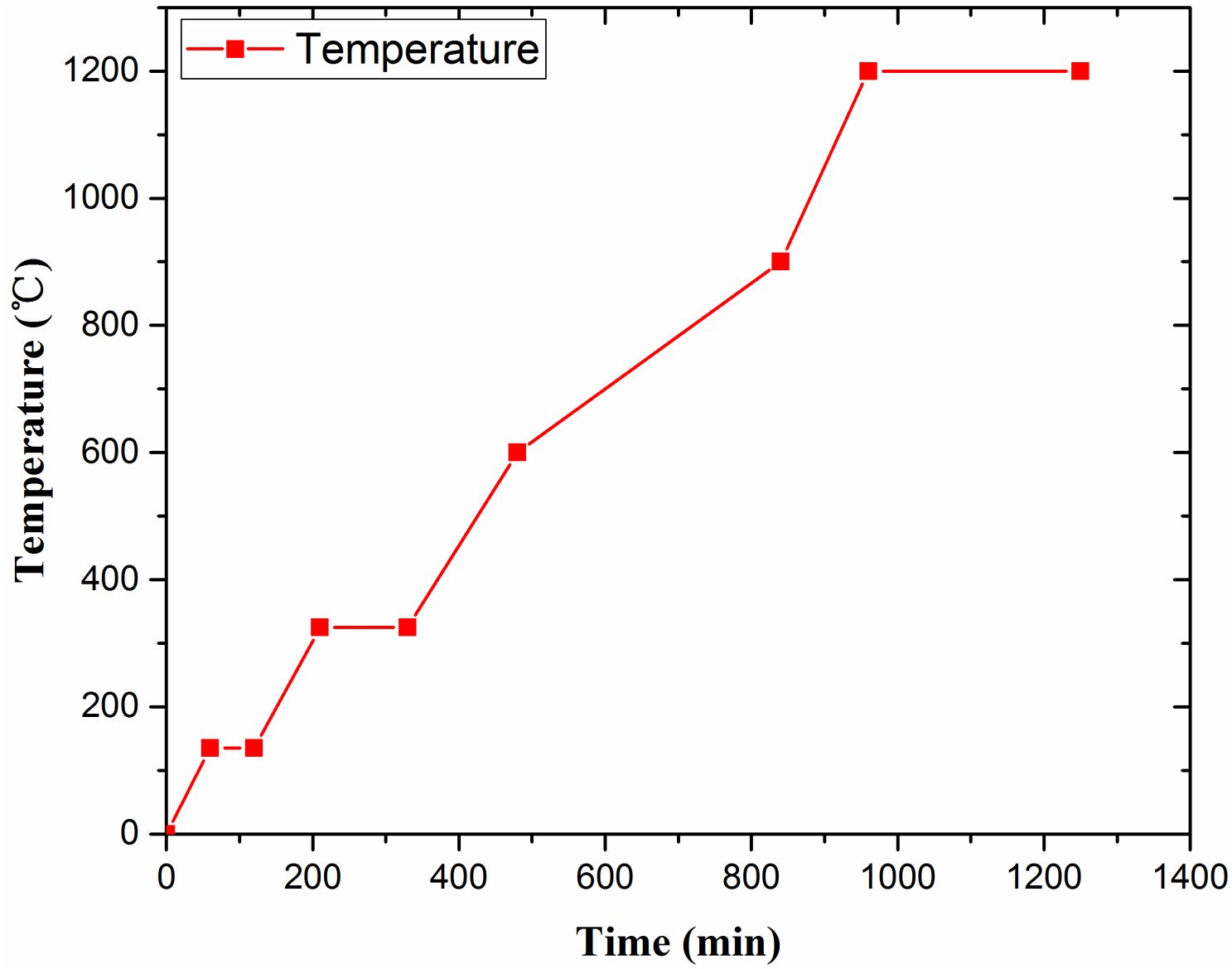

Figure 8

Sintering curve of supports

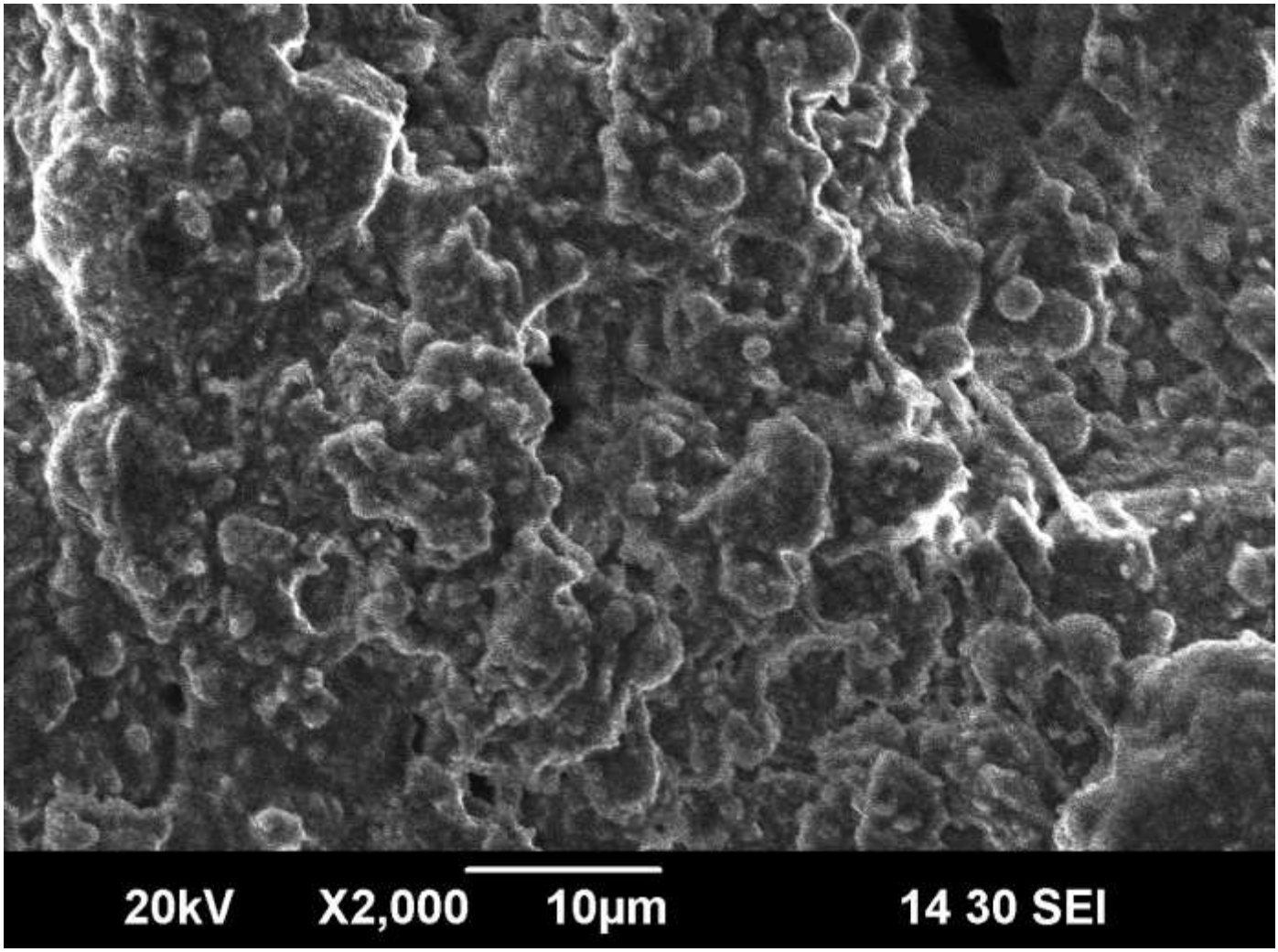

Figure 9

SEM image of support surface magnified 2000 times

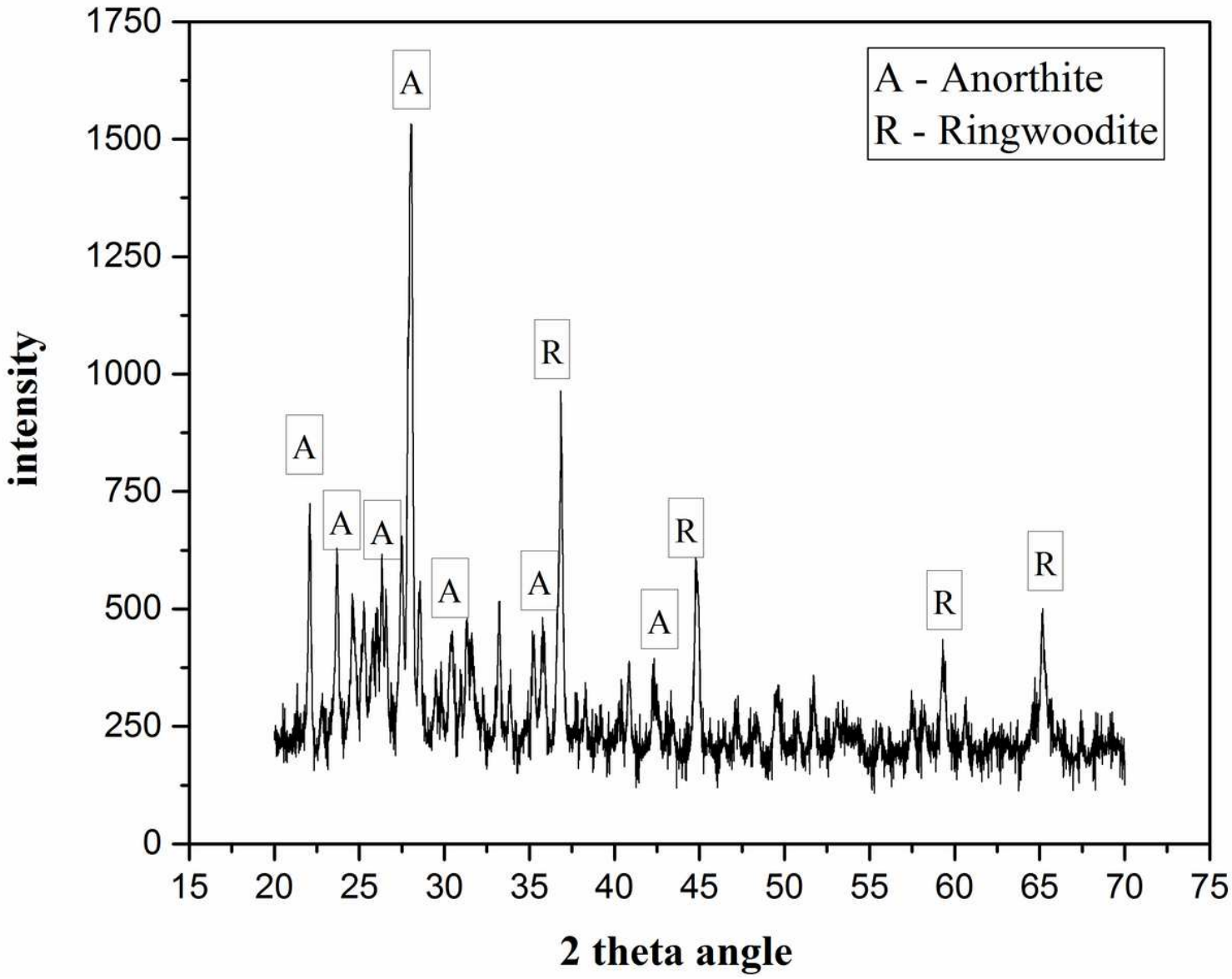

Figure 10

XRD pattern of fly ash based support

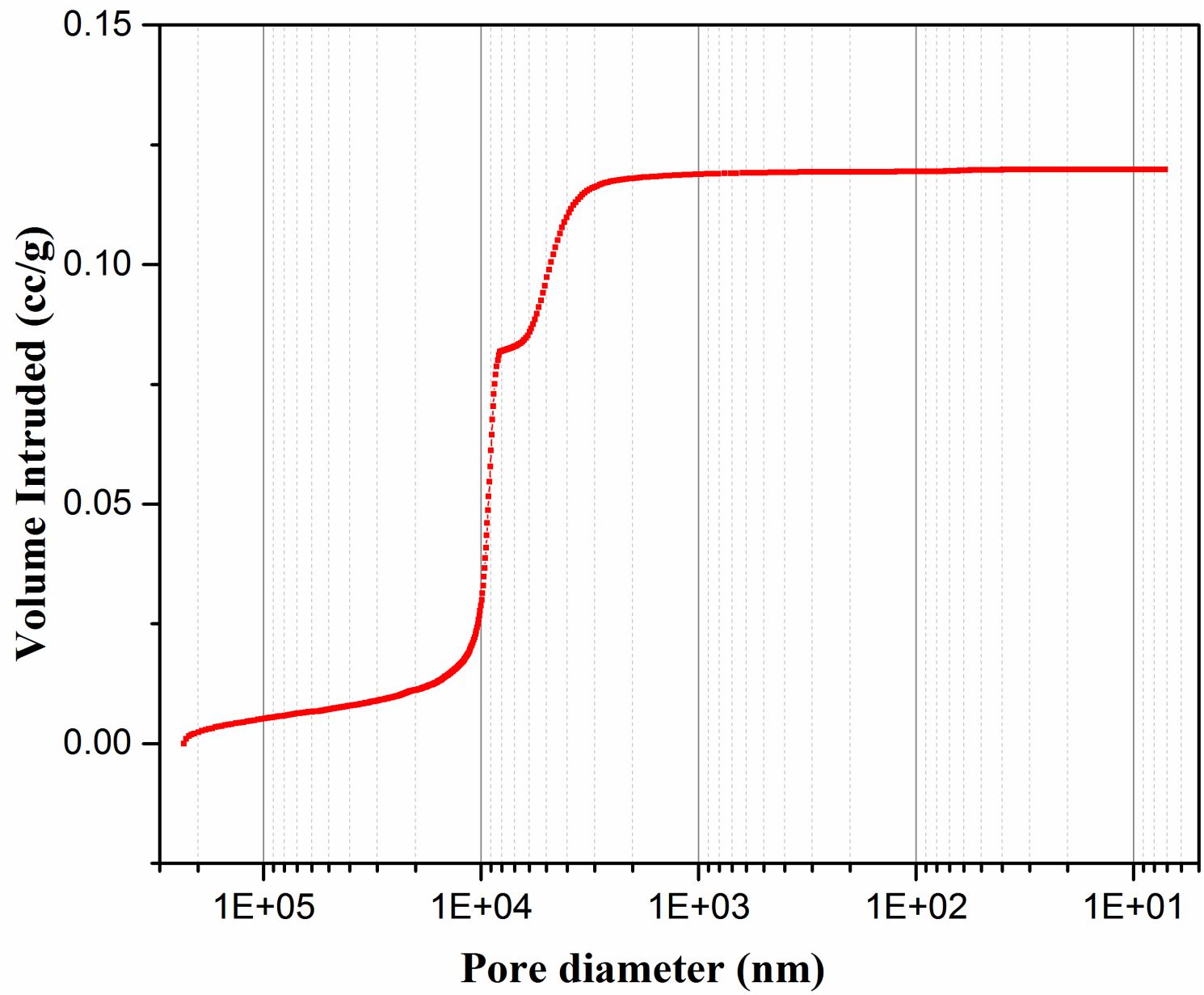

Figure 11

Mercury adsorption curve of talcum-fly ash support

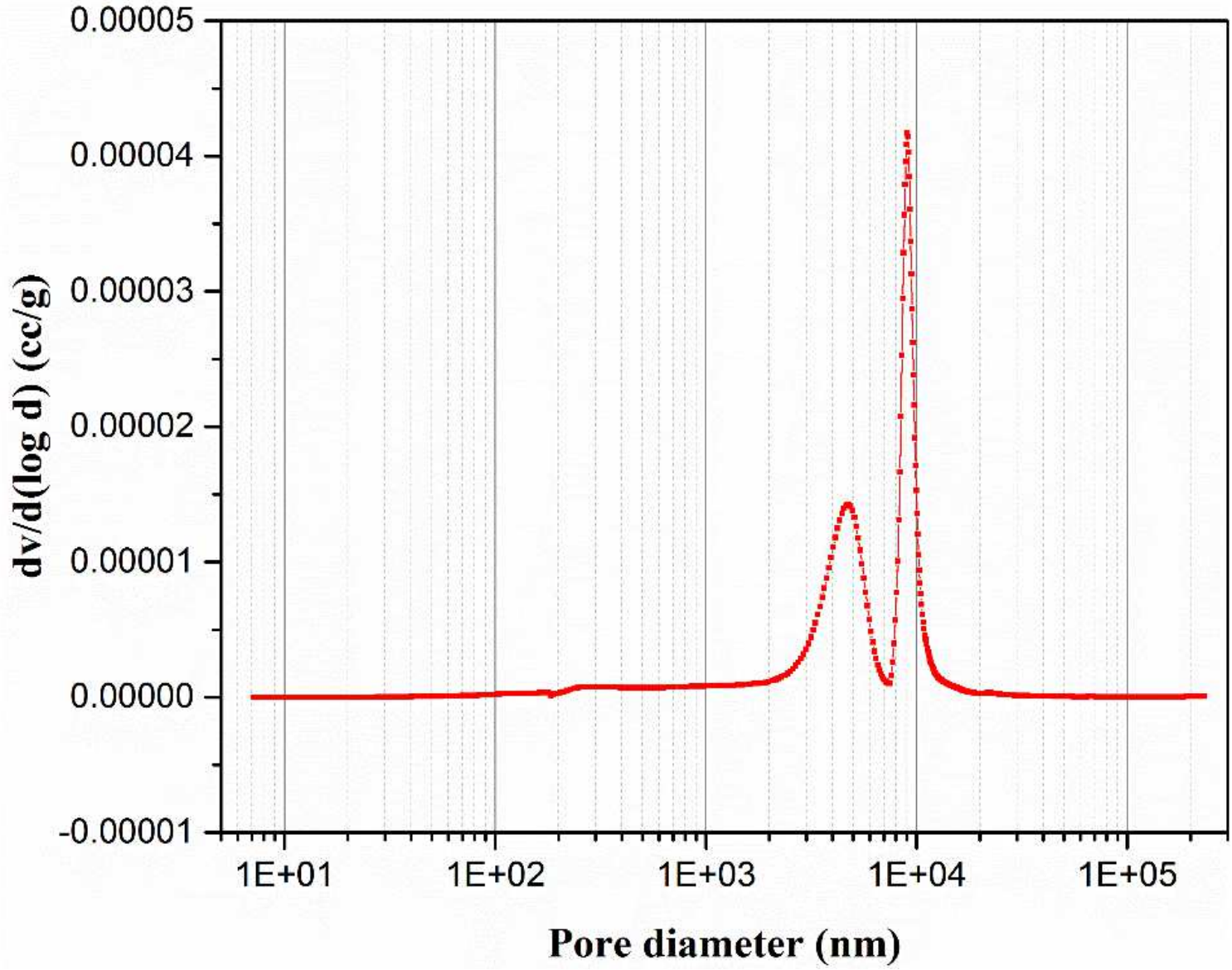

Figure 12

Pore diameter distribution curve of talcum-fly ash support

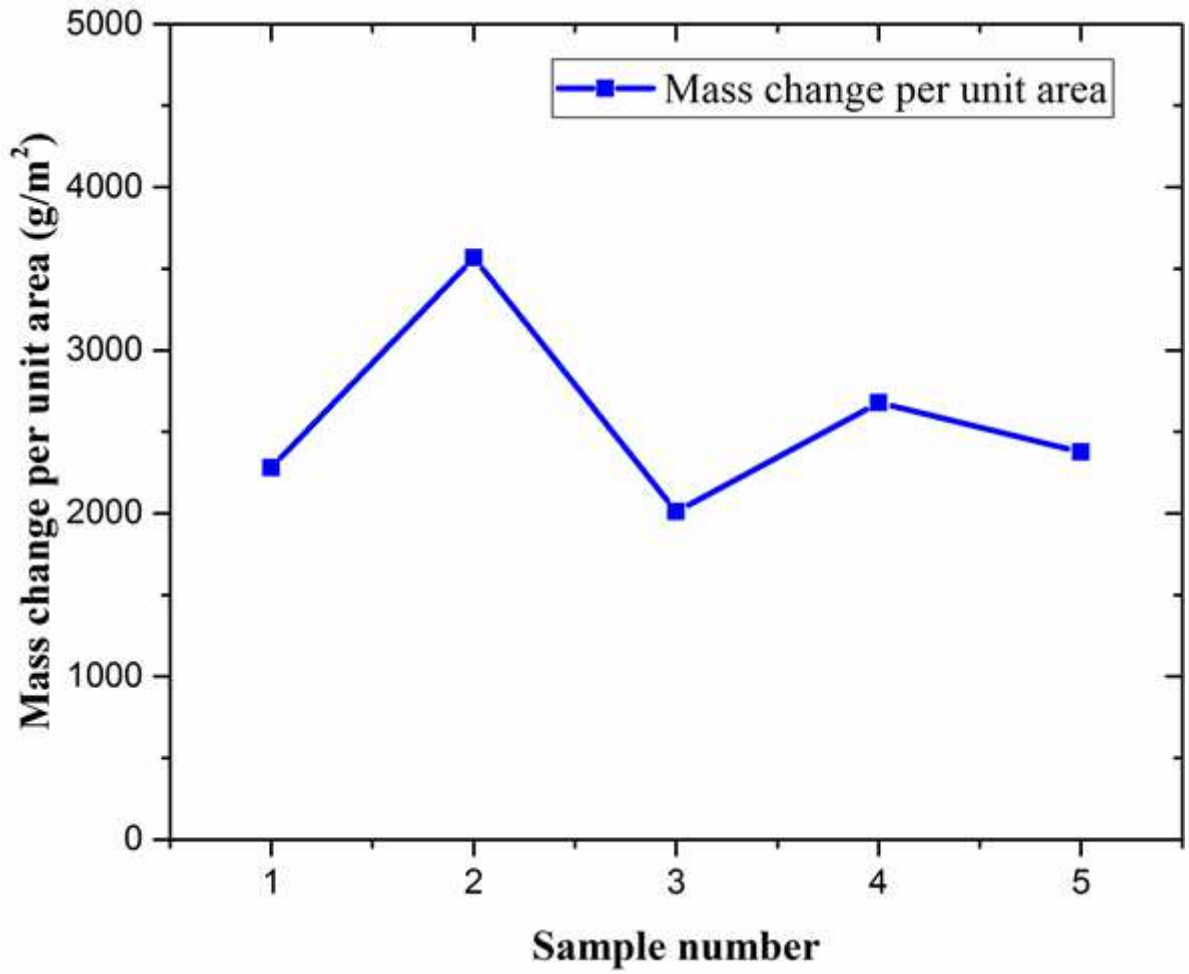

Figure 13

Mass change of unit area before and after corrosion

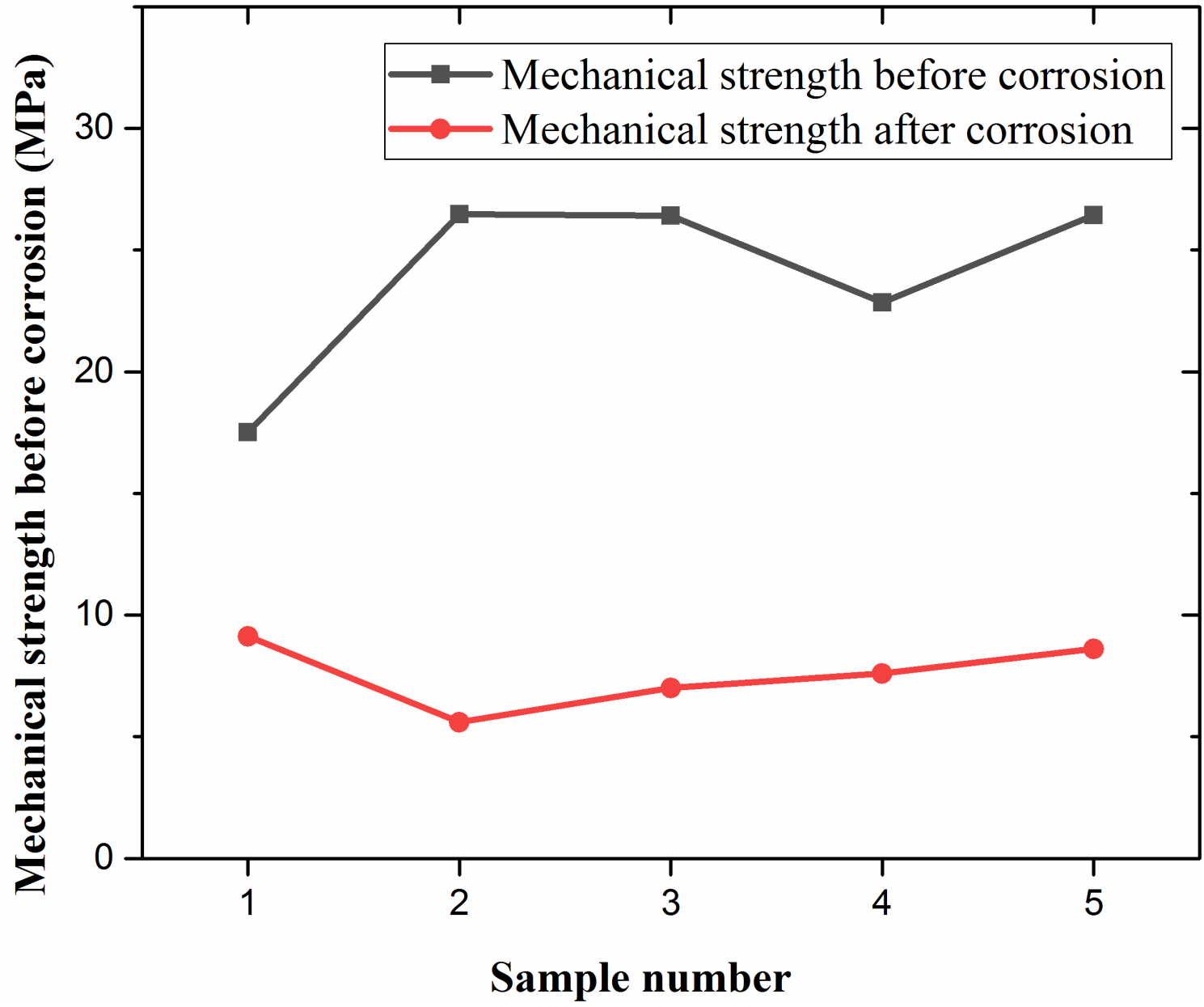

Figure 14

Change of mechanical strength of support before and after corrosion

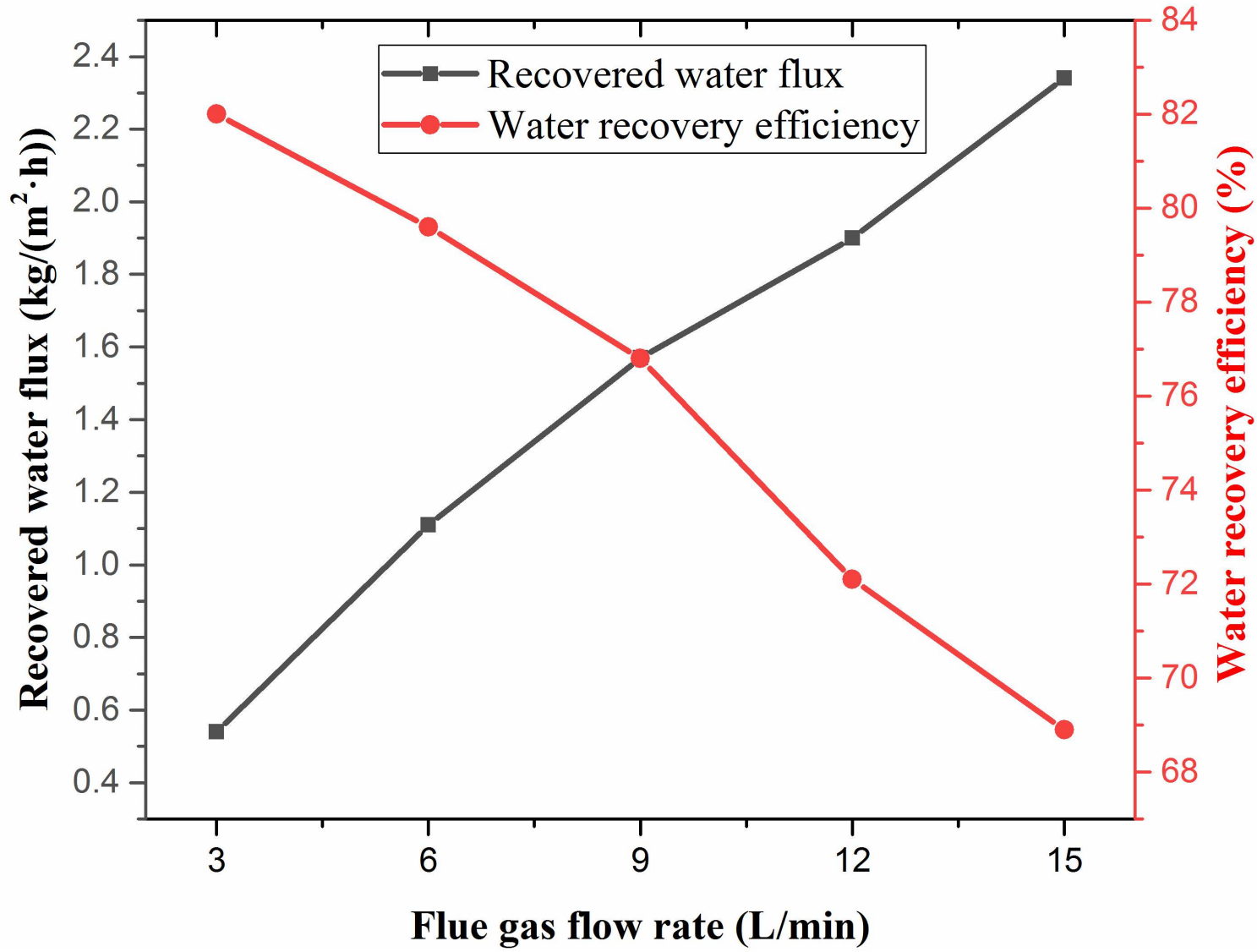

Figure 15

Effect of flue gas flow rate on water recovery performance (Experiment conditions: flue gas temperature 50 °C, cooling water flow rate 1 L/min, cooling water temperature 20 °C)

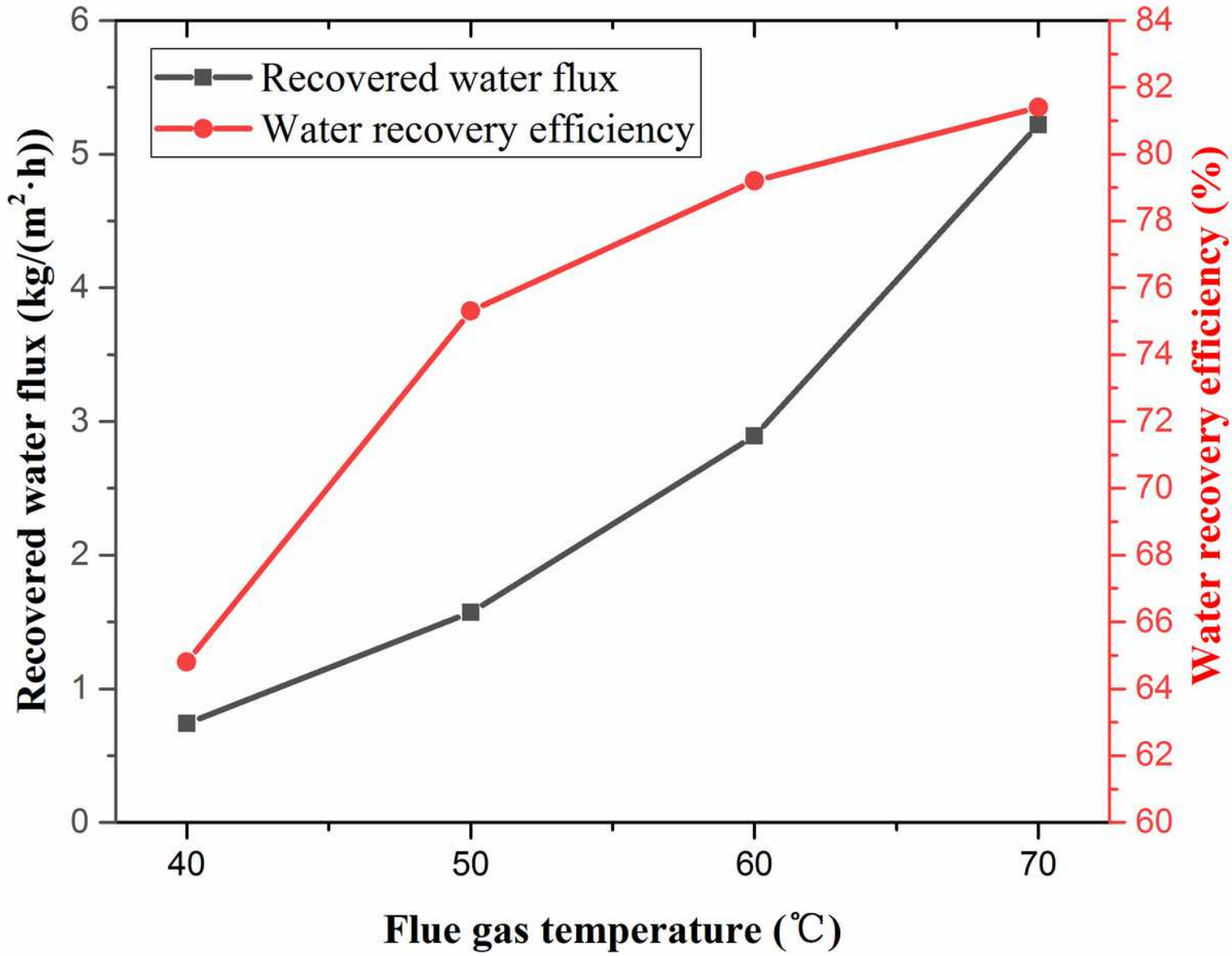

Figure 16

Effect of flue gas temperature on water recovery performance (Experiment conditions: flue gas flow 9 L/min, cooling water flow rate 1 L/min, cooling water temperature 20 °C)

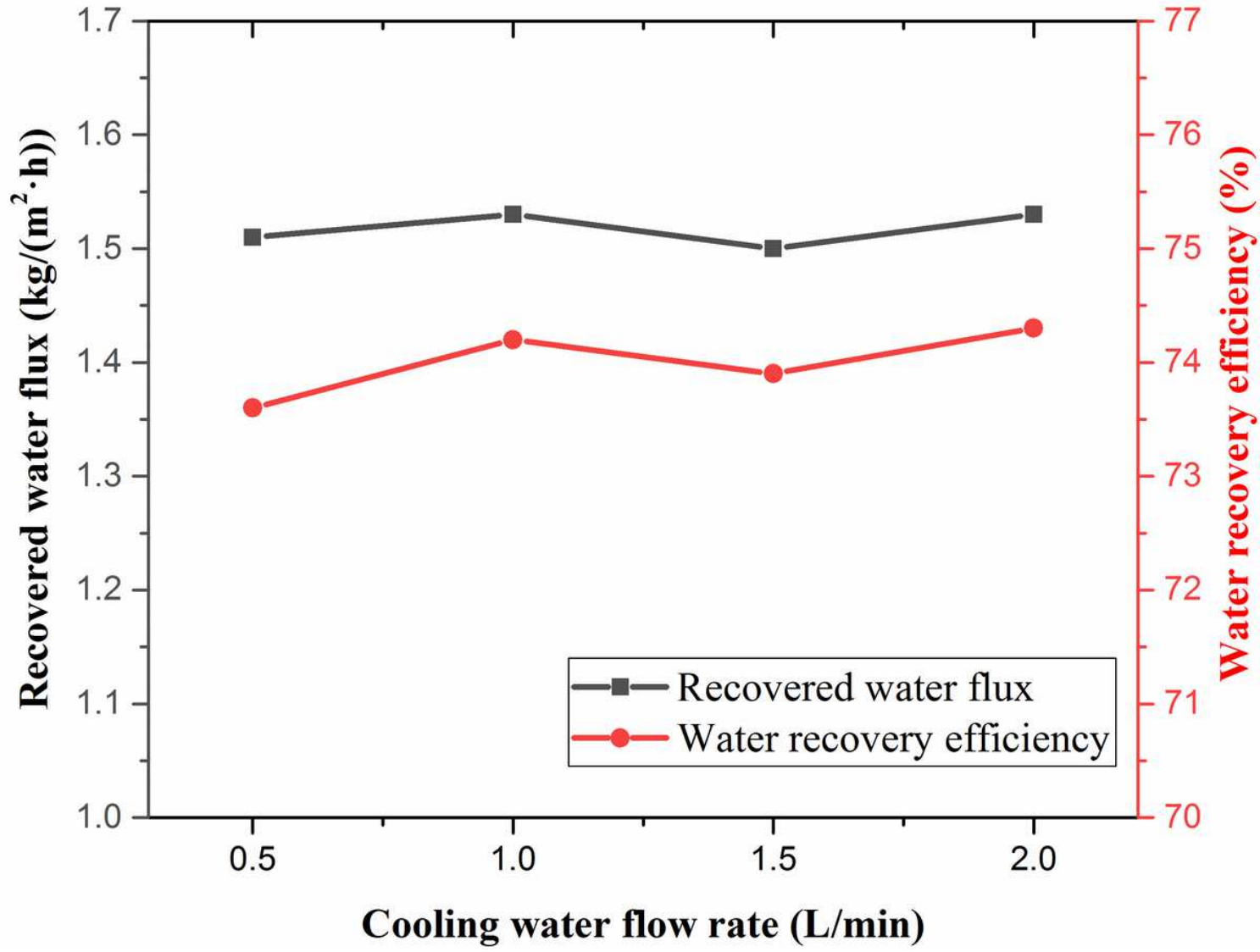

Figure 17

Effect of cooling water flow on water recovery performance (Experiment conditions: flue gas flow rate 9 L/min, flue gas temperature 50 °C, cooling water temperature 20 °C)

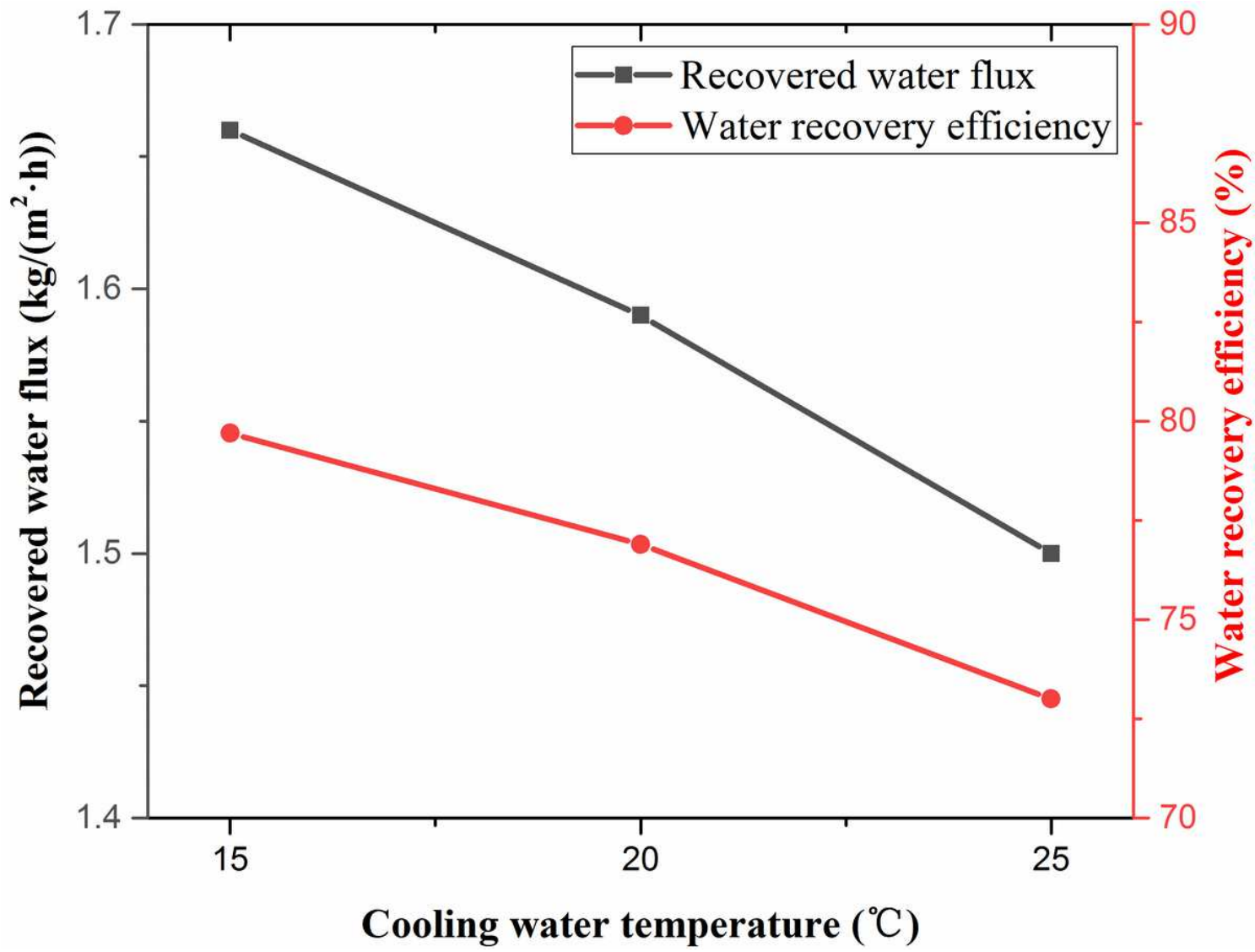

Figure 18

Effect of cooling water temperature on water recovery performance (Experiment conditions: flue gas flow rate 9 L/min, flue gas temperature 50 °C, cooling water flow 1 L/min)

Supplementary Files

This is a list of supplementary files associated with this preprint. Click to download.

- HighlightsStudyonthepreparation1214.docx